

Topological semimetal and superfluid of s -wave interacting fermionic atoms in an orbital optical lattice

Maksims Arzamasovs,¹ Shuai Li,¹ W. Vincent Liu,^{2,3,4,*} and Bo Liu^{1,†}

¹MOE Key Laboratory for Nonequilibrium Synthesis and Modulation of Condensed Matter, Shaanxi Province Key Laboratory of Quantum Information and Quantum Optoelectronic Devices, School of Physics, Xi'an Jiaotong University, Xi'an 710049, China

²Department of Physics and Astronomy, University of Pittsburgh, Pittsburgh PA 15260, USA

³Wilczek Quantum Center, School of Physics and Astronomy and T. D. Lee Institute, Shanghai Jiao Tong University, Shanghai 200240, China

⁴Shanghai Research Center for Quantum Sciences, Shanghai 201315, China

Recent advanced experimental implementations of optical lattices with highly tunable geometry open up new regimes for quantum many-body states of matter that previously had not been accessible. Here we introduce a symmetry-based method of utilizing the geometry of optical lattice to systematically control topologically non-trivial orbital hybridization. Such an orbital mixing leads to an unexpected and yet robust topological semimetal at single-particle level for a gas of fermionic atoms. When considering s -wave attractive interaction between atoms as for instance tuned by Feshbach resonance, topological superfluid state with high Chern number is unveiled in the presence of on-site rotation. This state supports chiral edge excitations, manifesting its topological nature. An experimental realization scheme is designed, which introduces a systematic way of achieving a new universality class (such as Chern number of 2) of orbital-hybridized topological phases beyond geometrically standard optical lattices.

Pursuit of topological phases of matter is one of the central thrusts in condensed matter physics since the discovery of superfluid ^3He chiral A phase [1] and quantum Hall effect [2, 3]. The concept of topology not only plays a key role in a variety of exotic quantum phenomena, such as topological insulators, chiral superconductors or Weyl semimetals, but is also closely related to fundamental physics, i.e., to distinguish new phases of matter that cannot be characterized by broken symmetries. It has thus explosively triggered a tremendous amount of efforts in both theoretical and experimental studies in various solid state materials. Besides the continuously growing efforts in solids, there has been a great interest in simulating topological matter with ultracold gases. Such highly controllable atomic systems will not only provide a versatile tool for simulating electronic systems, but also supply new possibilities to study new phenomena with no counterpart in solids. Recent experimental advances in creating tunable spin-orbit coupling by using the Raman scheme provide unprecedented opportunities for the study of topological matter in ultracold gases [4–15]. Moreover, the hybridization of orbital bands with different parity has opened a completely different avenue to emulate spin-orbit coupling or artificial gauge fields in general for cold atoms [16–22], yielding various interesting quantum states of matter [23–29]. However, the way to systematically engineer the orbital-hybridized topological phases of matter in static optical lattices remains unclear and stands as an obstacle of a substantial effort.

In this work, we report the discovery of a new mechanism to explore various unexpected orbital-hybridized topological phases. To demonstrate this scheme, a concrete model of ultracold fermionic atoms in an optical lattice is introduced

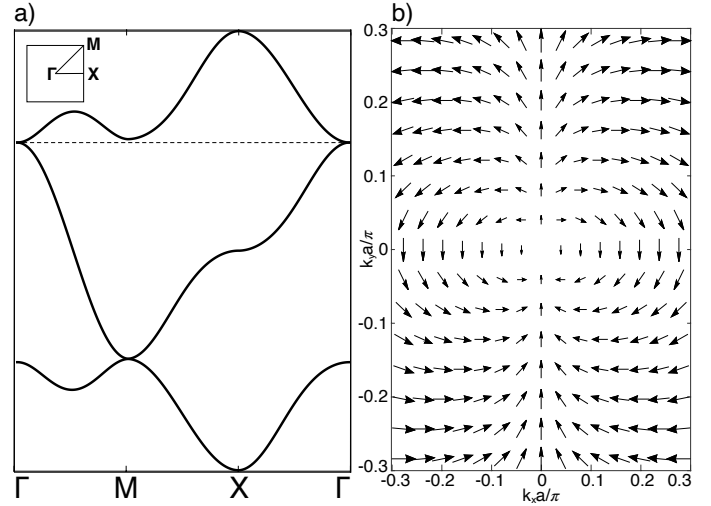


FIG. 1: (a) Single-particle energy spectrum of the tight-binding model in Eq. (1). We show the band structure along a contour in momentum space demonstrated in the inset of Fig. 1(a). The band degeneracy point appears at Γ with the parabolic dispersion. (b) The topological nature of band degeneracy point. The planar vector \mathbf{h} defined in Eq. (S4) forms a topological defect in (k_x, k_y) -plane, which is a vortex in the momentum space with winding number 2. Other parameters are chosen as $t_m = 0.6t_{\parallel}$ and $t_z = t_{\perp} = 0.3t_{\parallel}$.

below. The key idea here is to introduce the symmetry-based method of systematically controlling the non-trivial hybridization between degenerate orbitals of ultracold atoms in optical lattices. Surprisingly, we unveil that the interplay between manipulating the inversion symmetry of the system and orbital degeneracy of cold atoms in optical lattices can lead to a novel type of topologically non-trivial semimetal, where neither Raman-induced spin-orbit coupling nor other artificial gauge field is required. When further considering attrac-

*Electronic address: wvliu@pitt.edu

†Electronic address: liubophy@gmail.com

tion between fermionic atoms, an s-wave interaction induced topological superfluid with high Chern number emerges in the presence of on-site rotation. This idea is motivated by the recent experimental advances in manipulating higher orbital bands in optical lattices, such as the breakthrough observation of long-lived p -band bosonic atoms in a checkerboard lattice [19–22]. It provides unprecedented opportunities to investigate quantum many-body phases with orbital degrees of freedom [24, 25, 27–37]. As we shall show with the model below, the symmetry-based manipulation of non-trivial hybridization between degenerate orbitals can lead to other unexpected results.

Orbital-hybridized topological semimetal—Let us consider an ultracold fermionic gas loaded in a 2D optical lattice which can be realized from a strongly anisotropic 3D optical lattice. Specifically, the lattice potential can be expressed as $V_{\text{OL}}(\mathbf{r}) = -V_x \cos^2(k_{Lx}x) - V_y \cos^2(k_{Ly}y) - V_z \cos^2(k_{Lz}z)$ with the wavevectors of the laser fields k_{Lx} , k_{Ly} and k_{Lz} . The corresponding lattice constants are $a_x = \pi/k_{Lx}$, $a_y = \pi/k_{Ly}$, $a_z = \pi/k_{Lz}$ along the x , y and z directions, respectively. Here we focus on the case with lattice depth

$V_z \gg V_x = V_y$ and the system dynamically behaves as a 2D system. In the deep lattice limit, the lattice potential at each site can be approximated by a harmonic oscillator. Under this approximation, the requirement of $V_x k_{Lx}^2 = V_y k_{Ly}^2 = V_z k_{Lz}^2$ would keep the local SO(3) rotation symmetry at each lattice site, which guarantees the three-fold degeneracy of p -orbitals locally. Another key ingredient of our scheme is to include a magnetic field gradient along the z -direction. The single-particle physics can thus be captured by the following Hamiltonian, $H_0 = -\frac{\hbar^2}{2m} \nabla^2 + V_{\text{OL}}(\mathbf{r}) - \mathbf{F} \cdot \mathbf{r}$, where $\mathbf{F} = -J \nabla_z B$ is the force applied to the atom with spin magnetic moment J . Here we want to emphasize the key role of the external magnetic field gradient in our proposal. First, it breaks the inversion symmetry along the z -direction and thus induces the non-trivial hybridization between the degenerate orbitals, i.e., p_x and p_z , p_y and p_z orbitals. Second, tunneling in the z -direction is further suppressed by a linear tilt of the energy per lattice site, making the system dynamically 2D. The p -orbital fermions here can be described by the following multi-orbital model in the tight binding regime,

$$\begin{aligned} \mathbf{H}_0 = & t_{\parallel} \sum_{\mathbf{r}_i} C_{p_x}^{\dagger}(\mathbf{r}_i) C_{p_x}(\mathbf{r}_i + \vec{e}_x) - t_{\perp} \sum_{\mathbf{r}_i} C_{p_x}^{\dagger}(\mathbf{r}_i) C_{p_x}(\mathbf{r}_i + \vec{e}_y) + t_{\parallel} \sum_{\mathbf{r}_i} C_{p_y}^{\dagger}(\mathbf{r}_i) C_{p_y}(\mathbf{r}_i + \vec{e}_y) - \\ & t_{\perp} \sum_{\mathbf{r}_i} C_{p_y}^{\dagger}(\mathbf{r}_i) C_{p_y}(\mathbf{r}_i + \vec{e}_x) - t_z \sum_{\mathbf{r}_i} [C_{p_z}^{\dagger}(\mathbf{r}_i) C_{p_z}(\mathbf{r}_i + \vec{e}_x) + C_{p_z}^{\dagger}(\mathbf{r}_i) C_{p_z}(\mathbf{r}_i + \vec{e}_y)] + \\ & t_m \sum_{\mathbf{r}_i} [C_{p_x}^{\dagger}(\mathbf{r}_i + \vec{e}_x) C_{p_z}(\mathbf{r}_i) - C_{p_x}^{\dagger}(\mathbf{r}_i) C_{p_z}(\mathbf{r}_i + \vec{e}_x)] + \\ & t_m \sum_{\mathbf{r}_i} [C_{p_y}^{\dagger}(\mathbf{r}_i + \vec{e}_y) C_{p_z}(\mathbf{r}_i) - C_{p_y}^{\dagger}(\mathbf{r}_i) C_{p_z}(\mathbf{r}_i + \vec{e}_y)] + h.c., \end{aligned} \quad (1)$$

where $C_{\nu}^{\dagger}(\mathbf{r}_i)$ and $C_{\nu}(\mathbf{r}_i)$ with $\nu = p_x, p_y, p_z$, are fermionic creation and annihilation operators for the particle in the ν orbital at lattice site \mathbf{r}_i . t_{\parallel} is the longitudinal hopping and t_{\perp} is the corresponding transverse hopping. The relative signs of the hopping amplitudes are fixed by the parity of p_x and p_y orbitals. t_z describes the hopping of the p_z fermions in the xy -plane. The key ingredient in our model is the hybridization between the p_x and p_z , p_y and p_z orbitals, characterized by t_m in Eq. (1). Such hybridization between degenerate orbitals arises from the asymmetric shape of the p_z orbital wavefunction induced by the inversion symmetry breaking along the

z -direction, which is highly tunable through varying the magnetic field gradient as shown in Fig. S1 of the Supplemental Material (SM). In the momentum space, the single-particle Hamiltonian Eq. (1) can be rewritten as

$$\mathbf{H}_0(\mathbf{k}) = \begin{pmatrix} C_{p_x}^{\dagger}(\mathbf{k}) & C_{p_y}^{\dagger}(\mathbf{k}) & C_{p_z}^{\dagger}(\mathbf{k}) \end{pmatrix} \mathcal{H}(\mathbf{k}) \begin{pmatrix} C_{p_x}(\mathbf{k}) \\ C_{p_y}(\mathbf{k}) \\ C_{p_z}(\mathbf{k}) \end{pmatrix},$$

where

$$\mathcal{H}(\mathbf{k}) = \begin{pmatrix} 2t_{\parallel} \cos(k_x a) - 2t_{\perp} \cos(k_y a) & 0 & 2it_m \sin(k_x a) \\ 0 & 2t_{\parallel} \cos(k_y a) - 2t_{\perp} \cos(k_x a) & 2it_m \sin(k_y a) \\ -2it_m \sin(k_x a) & -2it_m \sin(k_y a) & -2t_z (\cos(k_x a) + \cos(k_y a)) \end{pmatrix}, \quad (2)$$

with $\mathbf{k} = (k_x, k_y)$ taking values in the first Brillouin zone

and $a \equiv a_x = a_y$. $C_{\nu}^{\dagger}(\mathbf{k})$ and $C_{\nu}(\mathbf{k})$ represent the ν -

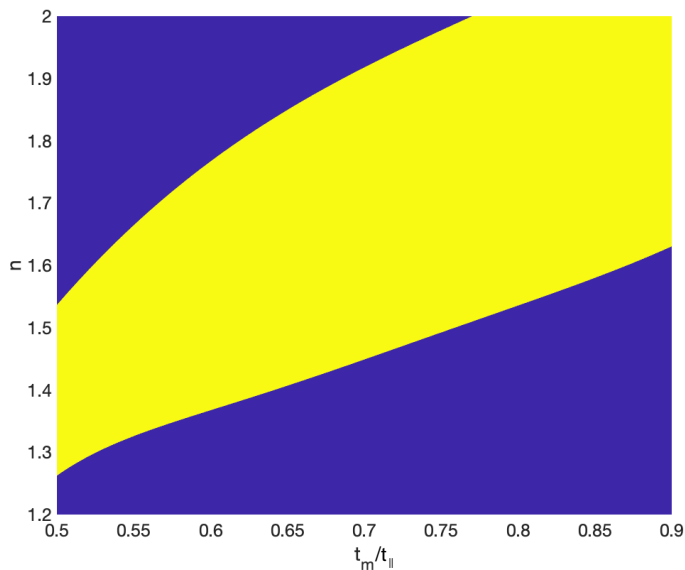


FIG. 2: Topological phase diagram as a function of orbital mixing strength t_m for different filling n of fermionic atoms in optical lattices. The topological non-trivial (yellow area) and trivial (purple area) superfluids are separated and the phase boundary corresponds with the closing of the bulk gap. Interestingly, the topological superfluid proposed here possesses high Chern number, i.e., $C = 2$. Other parameters are chosen as $|W| = 0.5t_{\parallel}$, $U = 3W$, $t_z = t_{\perp} = 0.2t_{\parallel}$ and $\Omega_z = 0.5t_{\parallel}$.

orbital fermionic creation and annihilation operators in momentum space, respectively. The eigenvalues of the 3×3 matrix in Eq. (2) give the single-particle band structure. As shown in Fig. 1(a), we find that the second and the third band cross at $\Gamma(k_x = 0, k_y = 0)$ point (the center of the Brillouin zone). Zooming into the vicinity of Γ shows that it develops a parabolic touching, which is qualitatively distinct from the linear Dirac or Weyl points. Surprisingly, such a band degeneracy point in our model behaves like a topological defect, i.e., a vortex with winding number 2, and thus an unexpected topological semimetal is developed. To show the topological nature of such a semimetal, we derive an effective low-energy theory around the band degeneracy point at Γ (see details in SM), captured by the following effective Hamiltonian

$$\mathbf{H}_{eff} = c_0 (k_x^2 + k_y^2) \mathbb{I}_{2 \times 2} + c_1 k_x k_y \sigma_x + c_3 (k_x^2 - k_y^2) \sigma_z, \quad (3)$$

where $c_0 = a^2[-t_{\parallel} + t_{\perp} + 2t_m^2/(t_{\parallel} - t_{\perp} + 2t_z)]/2$, $c_1 = 2t_m^2 a^2/(t_{\parallel} - t_{\perp} + 2t_z)$ and $c_3 = a^2[-t_{\parallel} - t_{\perp} + 2t_m^2/(t_{\parallel} - t_{\perp} + 2t_z)]/2$. ($\mathbb{I}_{2 \times 2}$, σ_x , σ_z) are the unit and Pauli matrices. To visualize the topological nontriviality of the quadratic touching point here, a 2D vector field $\mathbf{h}(\mathbf{k})$ can be defined from the coefficients of the two Pauli matrices in \mathbf{H}_{eff} as

$$\mathbf{h}(\mathbf{k}) = (c_1 k_x k_y, c_3 (k_x^2 - k_y^2)). \quad (4)$$

As shown in Fig. 1(b), the vector field $\mathbf{h}(\mathbf{k})$ forms a vortex structure in the momentum space. At the vortex core, the length of the vector vanishes, indicating that the band gap vanishes at the band degeneracy point. Therefore, such a band-touching point forms a topological defect. Its topological nature is also confirmed from the calculation of the winding number (see details in SM) and it turns out that the winding number is 2, which is distinct from the linear Dirac point with winding number 1. In fact, the band degeneracy point here is protected by the lattice rotation C_4 and reflection symmetries, where the reflection in the horizontal and vertical directions are associated with the transformations of fermionic operators as $\mathcal{R}_{\parallel} \equiv \{C_{p_x}(\mathbf{r}_i) \rightarrow -C_{p_x}(-\mathbf{r}_{ix}, \mathbf{r}_{iy}), C_{p_y(z)}(\mathbf{r}_i) \rightarrow C_{p_y(z)}(-\mathbf{r}_{ix}, \mathbf{r}_{iy})\}$ and $\mathcal{R}_{\perp} \equiv \{C_{p_x(z)}(\mathbf{r}_i) \rightarrow C_{p_x(z)}(\mathbf{r}_{ix}, -\mathbf{r}_{iy}), C_{p_y}(\mathbf{r}_i) \rightarrow -C_{p_y}(\mathbf{r}_{ix}, -\mathbf{r}_{iy})\}$, respectively. Those associated with the $\pi/2$ -lattice rotation can be expressed as $C_{p_x(z)}(\mathbf{r}_i) \rightarrow C_{p_y(z)}(-\mathbf{r}_{iy}, \mathbf{r}_{ix}), C_{p_y}(\mathbf{r}_i) \rightarrow -C_{p_x}(-\mathbf{r}_{iy}, \mathbf{r}_{ix})$. Here we would like to emphasize that the essential ingredient of our proposed topological semimetal arises from the non-trivial hybridization between different orbitals. The key idea in our scheme is to utilize the unique and intrinsic anisotropic spatial nature of higher orbitals. Through simply employing a magnetic field gradient to break the spatial inversion symmetry, the topologically non-trivial mixing between orbitals is thus induced, resulting in a substantially novel way of producing the topological semimetal in the ultracold atom based system.

S-wave interaction induced topological superfluid with high Chern number— In the previous section, it is shown that the non-trivial orbital mixing produces a topological band featured with the quadratic topological defect. Past studies show that it is unstable to the repulsive interaction, resulting in various topological phases, such as topological insulators and nematic phases [23, 38–41]. However, when considering the instability driven by the attraction, the singlet superconducting pairing is absent [41, 42]. Here we show that when adding a new ingredient, i.e., on-site rotation, a new type of topological superfluid with high Chern number can be created via the s -wave attraction induced singlet pairing. It thus opens up a new thrust towards exploring topological superfluids directly from an s -wave interaction, yet without requiring Raman-induced spin-orbit coupling nor other artificial gauge field. To illustrate this, let us consider loading spin-1/2 attractive fermionic atoms into the lattice system described above. With the addition of on-site rotation, the interacting model can be expressed as

$$\mathbf{H} = \mathbf{H}_{0,\sigma} + \mathbf{H}_{int} + \mathbf{H}_L. \quad (5)$$

The interaction part \mathbf{H}_{int} is

$$\begin{aligned} \mathbf{H}_{int} = & \sum_{\mathbf{r}_i} \left\{ U \sum_{\nu} n(\mathbf{r}_i)_{\nu,\uparrow} n(\mathbf{r}_i)_{\nu,\downarrow} + W \sum_{\nu \neq \rho} [n(\mathbf{r}_i)_{\nu,\uparrow} n(\mathbf{r}_i)_{\rho,\downarrow} + C_{\nu,\uparrow}^\dagger(\mathbf{r}_i) C_{\rho,\downarrow}^\dagger(\mathbf{r}_i) C_{\nu,\downarrow}(\mathbf{r}_i) C_{\rho,\uparrow}(\mathbf{r}_i) \right. \\ & \left. + C_{\nu,\uparrow}^\dagger(\mathbf{r}_i) C_{\nu,\downarrow}^\dagger(\mathbf{r}_i) C_{\rho,\downarrow}(\mathbf{r}_i) C_{\rho,\uparrow}(\mathbf{r}_i) \right\}, \end{aligned} \quad (6)$$

where the onsite particle number operator is defined as $n_{\nu,\sigma}(\mathbf{r}_i) \equiv C_{\nu,\sigma}^\dagger(\mathbf{r}_i) C_{\nu,\sigma}(\mathbf{r}_i)$ and $\nu, \rho = p_x, p_y, p_z$. The intra-orbital and inter-orbital interacting strength are captured by U and W , respectively. In general, $U \neq W$ which results from the anisotropic shape of p -orbitals. These onsite attraction strengths are determined by the effective s -wave scattering lengths, which can be tuned by means of the Feshbach resonance and lattice depth. $H_L = i\Omega_z \sum_{\mathbf{r}_i, \sigma} [C_{p_x, \sigma}^\dagger(\mathbf{r}_i) C_{p_y, \sigma}(\mathbf{r}_i) - C_{p_y, \sigma}^\dagger(\mathbf{r}_i) C_{p_x, \sigma}(\mathbf{r}_i)]$ is induced by the on-site rotation. Such an on-site rotation experiment has been achieved in a triangular optical lattice [43, 44] and the techniques are expected to be applicable to the model considered here. Through utilizing electro-optic phase modulators of the laser beams forming the lattice, we propose a method to realize the on-site rotation in our setup (see SM for details).

Due to the attractive interactions, the fermions tend to pair with each other and form a superfluid state at low temperatures. To study this superfluid state, we construct a path-integral formalism. The details are given in SM. The auxiliary complex bosonic fields $\Delta_{\nu\rho}^{(j)}(\mathbf{r}_i, \tau)$ and $\bar{\Delta}_{\nu\rho}^{(j)}(\mathbf{r}_i, \tau)$ with $\nu, \rho = p_x, p_y, p_z$ are introduced to obtain a bosonic effective action by Hubbard-Stratonovich transformation. Under the saddle-point approximation, the pairing order parameters $\Delta_{\nu\rho}$ can be determined (see details in SM). Surprisingly, we find that by simply tuning the average filling n of fermions in such a lattice system, the superfluids with distinct topological properties can be achieved. The topological nature of superfluidity here can be characterized by its non-trivial topological invariant. At mean-field level, the system can be described by the Bogoliubov-de Gennes (BdG) Hamiltonian (see SM for details). Since such a BdG Hamiltonian satisfies the particle-hole symmetry, i.e., $\Xi H_{BdG}(\mathbf{k}) \Xi^{-1} = -H_{BdG}^*(-\mathbf{k})$, with $\Xi \equiv \begin{pmatrix} 0 & \mathbb{I}_{3 \times 3} \\ \mathbb{I}_{3 \times 3} & 0 \end{pmatrix} \otimes \sigma_y$, the superfluid state predicted here belongs to the D symmetry class according to the general classification scheme of topological superconductors [45]. Therefore, its topology can be studied by evaluating the Chern number. Fig. 2 shows the topological phase diagram of the proposed superfluids. There are two different topological regions in the phase diagram, which are characterized by different Chern numbers. Intriguingly, a new topological orbital-hybridized superfluid with high Chern number, i.e., $C = 2$, is unveiled. For a fixed interaction strength, the system undergoes unusual type of topological phase transition from a topological trivial superfluid (SF) to the $C = 2$ topological non-trivial superfluid (tSF) when varying the filling of fermions. As shown in Fig. 2, the tSF phase region is quite sizable and would make the experimental realization easier.

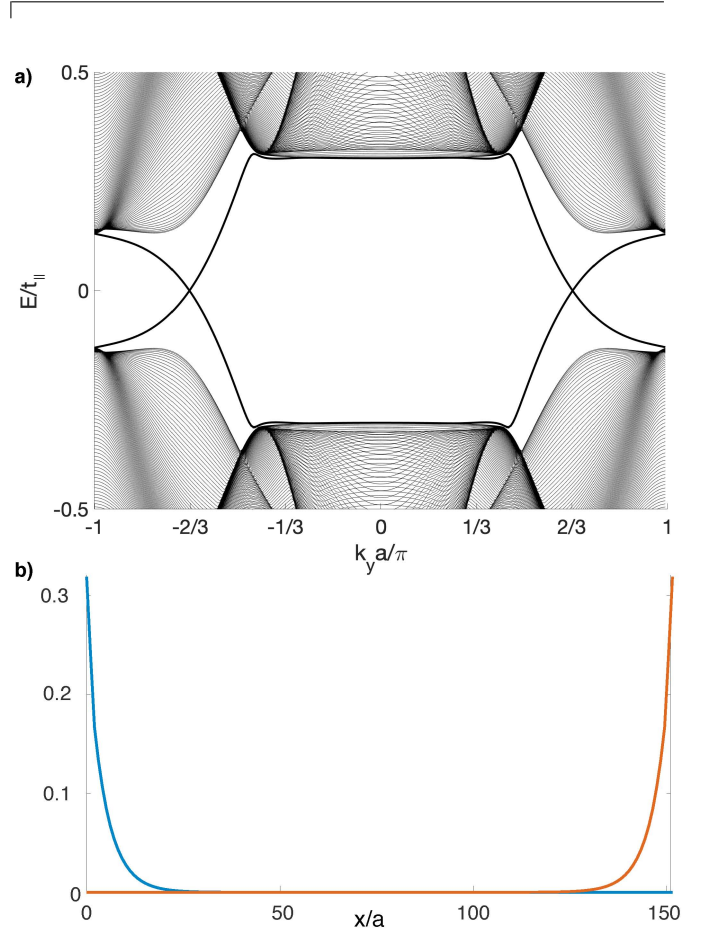


FIG. 3: (a) Energy spectrum of the Hamiltonian in Eq. (5) with open (periodic) boundary condition in the x (y) direction. There are two pairs of chiral modes located at the two outer edges, respectively. (b) The amplitudes of wavefunctions for the two chiral edge modes with $k_y a = 2\pi/3$ in (a). Here we choose $t_m = 0.8t_{\parallel}$ and $n = 1.6$. Other parameters are chosen as the same in Fig. 2.

To further demonstrate the topological nature of tSF phase, we shall show that the chiral edge modes are supported in this state. To see this, we consider a cylinder geometry of the system, where the open (periodic) boundary condition is chosen in the x (y) direction, respectively. The energy spectrum in Fig. 3 is labeled by momentum k_y . As shown in Fig. 3(a), all the bulk modes are gapped and there are two pairs of chiral edge states located at the two outer edges of the system, respectively, which are confirmed by the well-localized wavefunctions as shown in Fig. 3(b). It satisfies the so-called bulk-edge correspondence, since the Chern number of tSF state is 2. Since the number of chiral edge modes determines the quantized conductance in the system [2, 3], the high Chern num-

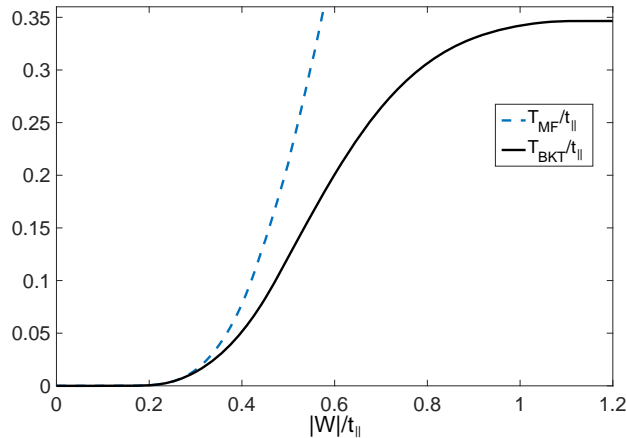


FIG. 4: BKT transition temperature T_{BKT} as a function of interaction strength. For comparison, the mean-field transition temperature T_{MF} is also shown here. We choose $t_m = 0.8t_{\parallel}$ and $n = 1.6$. Other parameters are the same as in Fig. 3.

bers are preferable in achieving more efficient edge channel transport. Therefore, our scheme would shed light on the new possibilities for edge-mode engineering through the fabrication of topological phases in both electronic solid state and atomic gas matter [46–50].

In the superfluid region, as the temperature increases, the system eventually undergoes a Berezinskii-Kosterlitz-Thouless (BKT) transition from the superfluid to normal state. At the BKT critical temperature [51, 52], the vortex-antivortex pairs disassociate and it costs zero free energy to generate a

single unbound vortex. The finite temperature phase diagram of our proposed system is obtained in Fig. 4 (see details in SM). In the current experiments, such as ^6Li or ^{40}K [53–57], taking advantage of the experimental realization of Feshbach resonance, the interaction is highly tunable. The BKT transition temperature can be estimated to reach around 40nK, making it promising to obtain the proposed tSF phase in experiments.

Conclusions — We have demonstrated a symmetry-based systematic method of engineering the non-trivial orbital hybridization in optical lattices. Various unexpected orbital-hybridized topological phases, including a topological semimetal with quadratic band touching, as well as a topological superfluid with high Chern number, are predicted through our proposed scheme. Moreover, this mechanism can be easily achieved in current experiments by utilizing our protocol of manipulating inversion symmetry in the optical lattice system, potentially circumventing the challenges in Raman-induced spin-orbit coupling scheme. The present approach thus complements with a new window to investigate topological phases in cold gases.

Acknowledgments This work is supported by the National Key Research and Development Program of China (2018YFA0307600), NSFC (Grant No. 12074305, 11774282, 11950410491), Cyrus Tang Foundation Young Scholar Program and the Fundamental Research Funds for the Central Universities (M. A., S. L. and B. L.), and by AFOSR Grant No. FA9550-16-1-0006, MURI-ARO Grant No. W911NF-17-1-0323 through UC Santa Barbara, and Shanghai Municipal Science and Technology Major Project (Grant No. 2019SHZDZX01) (W.V. L.).

-
- [1] G. E. Volovik, *The Universe in a Helium Droplet* (Oxford University Press, 2003).
 - [2] M. Z. Hasan and C. L. Kane, *Rev. Mod. Phys.* **82**, 3045 (2010).
 - [3] X.-L. Qi and S.-C. Zhang, *Rev. Mod. Phys.* **83**, 1057 (2011).
 - [4] V. Galitski and I. Spielman, *Nature (London)* **494**, 49 (2013).
 - [5] J. Dalibard, F. Gerbier, G. Juzeliūnas, and P. Öhberg, *Rev. Mod. Phys.* **83**, 1523 (2011).
 - [6] Y.-J. Lin, K. Jimenez-Garcia, and I. B. Spielman, *Nature (London)* **471**, 83 (2011).
 - [7] Z. Wu, L. Zhang, W. Sun, X.-T. Xu, B.-Z. Wang, S.-C. Ji, Y. Deng, S. Chen, X.-J. Liu, and J.-W. Pan, *Science* **354**, 83 (2016).
 - [8] L. W. Cheuk, A. T. Sommer, Z. Hadzibabic, T. Yefsah, W. S. Bakr, and M. W. Zwierlein, *Phys. Rev. Lett.* **109**, 095302 (2012).
 - [9] P. Wang, Z.-Q. Yu, Z. Fu, J. Miao, L. Huang, S. Chai, H. Zhai, and J. Zhang, *Phys. Rev. Lett.* **109**, 095301 (2012).
 - [10] G. Jotzu, M. Messer, R. Desbuquois, M. Lebrat, T. Uehlinger, D. Greif, and T. Esslinger, *Nature* **515**, 237 (2014).
 - [11] L. Duca, T. Li, M. Reitter, I. Bloch, M. Schleier-Smith, and U. Schneider, *Science* **347**, 288 (2015).
 - [12] M. Aidelsburger, M. Atala, M. Lohse, J. T. Barreiro, B. Paredes, and I. Bloch, *Phys. Rev. Lett.* **111**, 185301 (2013).
 - [13] H. Miyake, G. A. Siviloglou, C. J. Kennedy, W. C. Burton, and W. Ketterle, *Phys. Rev. Lett.* **111**, 185302 (2013).
 - [14] C. V. Parker, L.-C. Ha, and C. Chin, *Nat. Phys.* **9**, 769 (2013).
 - [15] H. Zhai, *Int. J. Mod. Phys. B* **26**, 1230001 (2012).
 - [16] S.-L. Zhang and Q. Zhou, *Phys. Rev. A* **90**, 051601 (2014).
 - [17] W. Zheng and H. Zhai, *Phys. Rev. A* **89**, 061603 (2014).
 - [18] S. K. Baur, M. H. Schleier-Smith, and N. R. Cooper, *Phys. Rev. A* **89**, 051605 (2014).
 - [19] T. Müller, S. Fölling, A. Widera, and I. Bloch, *Phys. Rev. Lett.* **99**, 200405 (2007).
 - [20] G. Wirth, M. Ölschläger, and A. Hemmerich, *Nat. Phys.* **7**, 147 (2011).
 - [21] P. Soltan-Panahi, D.-S. Lühmann, J. Struck, P. Windpassinger, and K. Sengstock, *Nat. Phys.* **8**, 71 (2012).
 - [22] T. Kock, M. Ölschläger, A. Ewerbeck, W.-M. Huang, L. Mathey, and A. Hemmerich, *Phys. Rev. Lett.* **114**, 115301 (2015).
 - [23] K. Sun, W. V. Liu, A. Hemmerich, and S. Das Sarma, *Nat. Phys.* **8**, 67 (2012).
 - [24] X. Li, E. Zhao, and W. V. Liu, *Nat. Commun.* **4**, 1523 (2013).
 - [25] B. Liu, X. Li, B. Wu, and W. V. Liu, *Nat. Commun.* **5**, 5064 (2014).
 - [26] B. Liu, P. Zhang, H. Gao, and F. Li, *Phys. Rev. Lett.* **121**, 015303 (2018).
 - [27] E. Zhao and W. V. Liu, *Phys. Rev. Lett.* **100**, 160403 (2008).

- [28] C. Wu, Phys. Rev. Lett. **100**, 200406 (2008).
 [29] C. Wu, Phys. Rev. Lett. **101**, 186807 (2008).
 [30] B. Liu, X. Li, and W. V. Liu, Phys. Rev. A **93**, 033643 (2016).
 [31] B. Liu, X. Li, R. G. Hulet, and W. V. Liu, Phys. Rev. A **94**, 031602(R) (2016).
 [32] Z. Zhang, H.-H. Hung, C. M. Ho, E. Zhao, and W. V. Liu, Phys. Rev. A **82**, 033610 (2010).
 [33] Z. Cai, Y. Wang, and C. Wu, Phys. Rev. A **83**, 063621 (2011).
 [34] Z. Cai, Y. Wang, and C. Wu, Phys. Rev. B **86**, 060517(R) (2012).
 [35] Z. Zhou, E. Zhao, and W. V. Liu, Phys. Rev. Lett. **114**, 100406 (2015).
 [36] F. Pinheiro, G. M. Bruun, J.-P. Martikainen, and J. Larson, Phys. Rev. Lett. **111**, 205302 (2013).
 [37] X. Li, Z. Zhang, and W. V. Liu, Phys. Rev. Lett. **108**, 175302 (2012).
 [38] K. Sun and E. Fradkin, Phys. Rev. B **78**, 245122 (2008).
 [39] V. Oganessian, S. A. Kivelson, and E. Fradkin, Phys. Rev. B **64**, 195109 (2001).
 [40] S. A. Kivelson, I. P. Bindloss, E. Fradkin, V. Oganessian, J. M. Tranquada, A. Kapitulnik, and C. Howald, Rev. Mod. Phys. **75**, 1201 (2003).
 [41] K. Sun, H. Yao, E. Fradkin, and S. A. Kivelson, Phys. Rev. Lett. **103**, 046811 (2009).
 [42] H.-X. Wang, Z.-H. Liu, and J.-H. Jiang, Chin. Phys. B **27**, 27402 (2018).
 [43] N. Gemelke, Ph.D. thesis, Stanford University (2007).
 [44] N. Gemelke, E. Sarajlic, and S. Chu, arXiv:1007.2677 (2010).
 [45] A. P. Schnyder, S. Ryu, A. Furusaki, and A. W. W. Ludwig, Phys. Rev. B **78**, 195125 (2008).
 [46] J. Röntynen and T. Ojanen, Phys. Rev. Lett. **114**, 236803 (2015).
 [47] J. Li, T. Neupert, Z. Wang, A. H. MacDonald, A. Yazdani, and B. A. Bernevig, Nat. Commun. **7**, 12297 (2016).
 [48] J. Röntynen and T. Ojanen, Phys. Rev. B **93**, 094521 (2016).
 [49] B. Huang, C. F. Chan, and M. Gong, Phys. Rev. B **91**, 134512 (2015).
 [50] Y. Yi-Xiang, F. Sun, and J. Ye, Phys. Rev. B **98**, 174506 (2018).
 [51] V. Berezinskii, Sov. Phys. JETP **34**, 610 (1972).
 [52] J. Kosterlitz and D. Thouless, J. Phys. C **6**, 1181 (1973).
 [53] C. A. Regal, M. Greiner, and D. S. Jin, Phys. Rev. Lett. **92**, 040403 (2004).
 [54] M. W. Zwierlein, C. A. Stan, C. H. Schunck, S. M. F. Raupach, A. J. Kerman, and W. Ketterle, Phys. Rev. Lett. **92**, 120403 (2004).
 [55] J. Kinast, S. L. Hemmer, M. E. Gehm, A. Turlapov, and J. E. Thomas, Phys. Rev. Lett. **92**, 150402 (2004).
 [56] M. Bartenstein, A. Altmeyer, S. Riedl, S. Jochim, C. Chin, J. H. Denschlag, and R. Grimm, Phys. Rev. Lett. **92**, 120401 (2004).
 [57] T. Bourdel, J. Cubizolles, L. Khaykovich, K. M. F. Magalhães, S. J. J. M. F. Kokkelmans, G. V. Shlyapnikov, and C. Salomon, Phys. Rev. Lett. **91**, 020402 (2003).
 [58] H. Feshbach, Ann. Phys. N. Y. **19**, 287 (1962).
 [59] D. Nelson and J. Kosterlitz, Phys. Rev. Lett. **39**, 1201 (1977).
 [60] T. Paananen, J. Phys. B **42**, 165304 (2009).
 [61] J. P. A. Devreese, J. Tempere, and C. A. R. S. de Melo, Phys. Rev. A **92**, 043618 (2015).
 [62] Y. Yanay and E. J. Mueller, arXiv:1209.2446 (2012).

Supplementary Material:

Topological semimetal and superfluid of s -wave interacting fermionic atoms in an orbital optical lattice

S-1. ORBITAL-HYBRIDIZED TOPOLOGICAL SEMIMETAL

In this section, we shall provide a detailed derivation of the effective Hamiltonian in Eq. (3). The method of Feshbach projectors [58] is used here to reduce the model in Eq. (2) to an effective low-energy Hamiltonian around the band touching point. The projection operators \mathbf{P} and $\mathbf{Q} = 1 - \mathbf{P}$ are introduced that project into the subspaces spanned by the two touching bands at the Γ point and the remaining band, respectively. The eigenvalue problem associated with the model Hamiltonian \mathbf{H}_0 can be written as $\mathbf{H}_0|\Psi\rangle = E|\Psi\rangle$, where $|\Psi\rangle$ is the eigenstate with eigenenergy E . The effective Hamiltonian \mathbf{H}_{eff} which describes the low-energy physics around the band touching point Γ can be obtained through

$$\left(\mathbf{P}\mathbf{H}_0\mathbf{P} + \mathbf{P}\mathbf{H}_0\mathbf{Q} \frac{1}{E - \mathbf{Q}\mathbf{H}_0\mathbf{Q}} \mathbf{Q}\mathbf{H}_0\mathbf{P} \right) \mathbf{P}|\Psi\rangle \equiv \mathbf{H}_{eff}\mathbf{P}|\Psi\rangle = E\mathbf{P}|\Psi\rangle. \quad (\text{S1})$$

By computing the relevant matrix elements of Eq. (S1) in the projected Hilbert space, the effective Hamiltonian \mathbf{H}_{eff} can be further expressed as

$$\mathbf{H}_{eff} = \begin{pmatrix} 2t_{\parallel} \cos(k_x a) - 2t_{\perp} \cos(k_y a) & 0 \\ 0 & 2t_{\parallel} \cos(k_y a) - 2t_{\perp} \cos(k_x a) \end{pmatrix} + \frac{2t_m^2}{t_{\parallel} - t_{\perp} + 2t_z (\cos(k_x a) + \cos(k_y a))} \begin{pmatrix} \sin^2(k_x a) & \sin(k_x a) \sin(k_y a) \\ \sin(k_x a) \sin(k_y a) & \sin^2(k_y a) \end{pmatrix}. \quad (\text{S2})$$

Expanding Eq. (S2) up to the second order in momentum near the Γ point, \mathbf{H}_{eff} can be further approximated as

$$\mathbf{H}_{eff}(k_x, k_y) \approx c_0 (k_x^2 + k_y^2) \mathbb{I}_{2 \times 2} + c_1 k_x k_y \sigma_x + c_3 (k_x^2 - k_y^2) \sigma_z, \quad (\text{S3})$$

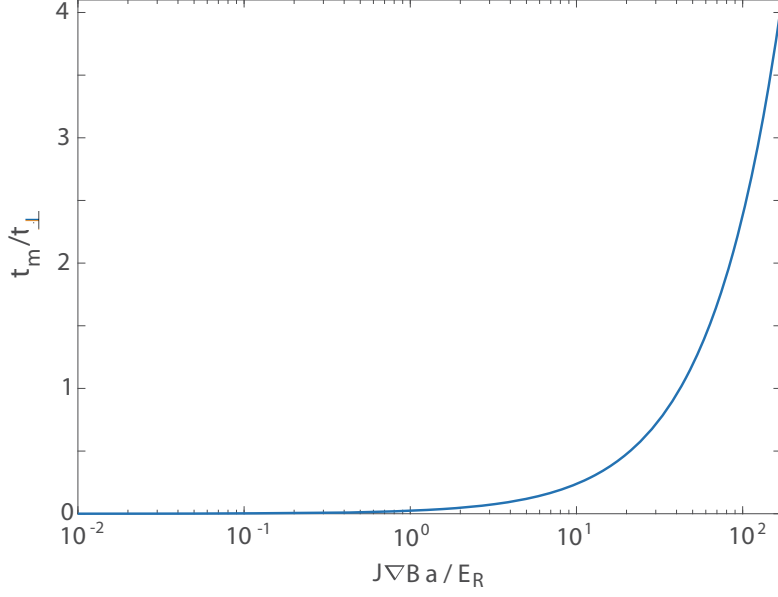


FIG. S1: The orbital hybridization t_m/t_\perp as a function of the magnetic field gradient. Here E_R is the recoil energy defined as $E_R = \frac{\hbar^2 k_L^2}{2m}$.

where $c_0 = \frac{a^2}{2} \left(-t_\parallel + t_\perp + \frac{2t_m^2}{t_\parallel - t_\perp + 2t_z} \right)$, $c_1 = \frac{2t_m^2 a^2}{t_\parallel - t_\perp + 2t_z}$, and $c_3 = \frac{a^2}{2} \left(-t_\parallel - t_\perp + \frac{2t_m^2}{t_\parallel - t_\perp + 2t_z} \right)$. σ_x , σ_z are the Pauli matrices and $\mathbb{I}_{2 \times 2}$ is the unit matrix. Eq. (S3) can also be parameterized by a vector in the (k_x, k_y) -plane as

$$\mathbf{h}(\mathbf{k}) = (c_1 k_x k_y, c_3 (k_x^2 - k_y^2)). \quad (\text{S4})$$

The vector $\mathbf{h}(k_x, k_y)$ defined here has a vortex structure with the winding number $W = \oint_C \frac{d\mathbf{k}}{2\pi} \left[\frac{h_x}{|\mathbf{h}|} \nabla \left(\frac{h_y}{|\mathbf{h}|} \right) - \frac{h_y}{|\mathbf{h}|} \nabla \left(\frac{h_x}{|\mathbf{h}|} \right) \right]$ being equal to 2.

S-2. LOCAL ROTATION

Through putting electro-optic modulators on the laser beams forming the lattice [43, 44], the lattice potential can be expressed as

$$V(x, y, z) = -\frac{V}{2} [\cos^2(k_L x + \phi_x(t)) + \cos^2(k_L y + \phi_y(t))] - \frac{V}{4} [\cos^2(k_L x + k_L y + \phi_+(t)) + \cos^2(k_L x - k_L y + \phi_-(t))] - V_z \cos^2(k_L z), \quad (\text{S5})$$

where $V \equiv V_x = V_y$, $k_L \equiv k_{L_x} = k_{L_y}$ and the electro-optic phase modulators $\phi_x(t) = \Delta\phi \cos(\Omega_z t) \cos(\omega_{RF} t)$, $\phi_y(t) = \Delta\phi \cos(\Omega_z t + \pi/2) \cos(\omega_{RF} t)$, $\phi_+(t) = \Delta\phi \cos(\Omega_z t + \pi/4) \cos(\omega_{RF} t)$, $\phi_-(t) = \Delta\phi \cos(\Omega_z t - \pi/4) \cos(\omega_{RF} t)$ with the slow precession frequency Ω_z , the amplitude of oscillation $\Delta\phi$ and the fast rotation frequency ω_{RF} at radio frequency. It results in a periodical overall translation of the lattice at a radio-frequency ω_{RF} . Atoms do not follow the fast oscillation at radio frequency ω_{RF} and only feel a time averaged potential. The local potential near each site minimum in the rotating frame with frequency Ω_z can be approximately (dropping a constant) expressed as

$$V(x', y', z) \approx -\frac{3V}{2} \left(1 - \frac{\Delta\phi^2}{4} \right) + \frac{m\omega'^2 r'^2}{2} (1 + 2\epsilon \cos(2\phi')) + V_z k_{L_z}^2 z^2, \quad (\text{S6})$$

where $\frac{m\omega'^2}{2} = V k_L^2 \left(1 - \frac{\Delta\phi^2}{2} \right)$, $\epsilon = -\frac{\Delta\phi^2}{8(1 - \Delta\phi^2/2)}$, $r'^2 = x'^2 + y'^2$ and ϕ' is the polar angle of \mathbf{r}' . The reference frame with rotating axis along z -direction and angular velocity Ω_z with respect to the original frame can be captured by the following transformation $\begin{pmatrix} x' \\ y' \end{pmatrix} = \begin{pmatrix} \cos(\Omega_z t) & -\sin(\Omega_z t) \\ \sin(\Omega_z t) & \cos(\Omega_z t) \end{pmatrix} \begin{pmatrix} x \\ y \end{pmatrix}$. The slight deformation of the optical potential processes around each site center, i.e., the fourth term in Eq. (S6), which can be regarded as an on-site rotation [43, 44].

S-3. PATH INTEGRAL FORMALISM

By introducing Grassmann fields $\bar{C}_{\mu(\nu),\sigma}(\mathbf{r}_i, \tau)$, $C_{\mu(\nu),\sigma}(\mathbf{r}_i, \tau)$ with $\mu(\nu) = p_x, p_y, p_z$ and $\sigma = \uparrow, \downarrow$, which represent fermionic fields, the partition function of the system can be expressed as (the units are chosen as $\hbar = k_B = 1$)

$$\mathcal{Z} = \int \mathcal{D}\bar{C}\mathcal{D}C \exp(-S[\bar{C}, C]), \quad (\text{S7})$$

with the action S

$$S = S_0[\bar{C}, C] + S_{int}[\bar{C}, C], \quad (\text{S8})$$

where

$$S_0[\bar{C}, C] = \int_0^\beta d\tau \sum_{\mu\nu\mathbf{r}_i\mathbf{r}'_i\sigma} \bar{C}_{\mu,\sigma}(\mathbf{r}_i, \tau) \left(\delta_{\mu\nu} \delta_{\mathbf{r}_i, \mathbf{r}'_i} \partial_\tau + \mathcal{H}_{\mu\nu} \right) C_{\nu,\sigma}(\mathbf{r}'_i, \tau),$$

$$\begin{aligned} S_{int}[\bar{C}, C] = & W \int_0^\beta d\tau \sum_{\mathbf{r}_i} \left\{ 3 \sum_{\mu} \bar{C}_{\mu,\uparrow}(\mathbf{r}_i, \tau) \bar{C}_{\mu,\downarrow}(\mathbf{r}_i, \tau) C_{\mu,\downarrow}(\mathbf{r}_i, \tau) C_{\mu,\uparrow}(\mathbf{r}_i, \tau) \right. \\ & + \sum_{\mu \neq \nu} \bar{C}_{\mu,\uparrow}(\mathbf{r}_i, \tau) \bar{C}_{\mu,\downarrow}(\mathbf{r}_i, \tau) C_{\nu,\downarrow}(\mathbf{r}_i, \tau) C_{\nu,\uparrow}(\mathbf{r}_i, \tau) + \sum_{\mu \neq \nu} \bar{C}_{\mu,\uparrow}(\mathbf{r}_i, \tau) \bar{C}_{\nu,\downarrow}(\mathbf{r}_i, \tau) C_{\mu,\downarrow}(\mathbf{r}_i, \tau) C_{\nu,\uparrow}(\mathbf{r}_i, \tau) \\ & \left. + \sum_{\mu \neq \nu} \bar{C}_{\mu,\uparrow}(\mathbf{r}_i, \tau) \bar{C}_{\nu,\downarrow}(\mathbf{r}_i, \tau) C_{\nu,\downarrow}(\mathbf{r}_i, \tau) C_{\mu,\uparrow}(\mathbf{r}_i, \tau) \right\}, \end{aligned} \quad (\text{S9})$$

with assuming $U = 3W$.

The quartic fermionic interaction term in action S can be decoupled by introducing Hubbard-Stratonovich fields

$$\bar{\Delta}_{\mu\nu}^{(j)}(\mathbf{r}_i, \tau) \quad \text{and} \quad \Delta_{\mu\nu}^{(j)}(\mathbf{r}_i, \tau), \quad \text{where} \quad j = \begin{cases} 1, & \mu = \nu \\ 1, 2 & \mu \neq \nu \end{cases} \quad \text{and} \quad \mu, \nu = p_x, p_y, p_z. \quad (\text{S10})$$

Then the interaction part in the partition function can be rewritten as follows

$$\begin{aligned} & \int \mathcal{D}\bar{C}\mathcal{D}C \exp \left(-W \int_0^\beta d\tau \sum_{\mathbf{r}_i} \left\{ 3 \sum_{\mu} \bar{C}_{\mu,\uparrow}(\mathbf{r}_i, \tau) \bar{C}_{\mu,\downarrow}(\mathbf{r}_i, \tau) C_{\mu,\downarrow}(\mathbf{r}_i, \tau) C_{\mu,\uparrow}(\mathbf{r}_i, \tau) \right. \right. \\ & \quad \left. \left. + \sum_{\mu \neq \nu} \bar{C}_{\mu,\uparrow}(\mathbf{r}_i, \tau) \bar{C}_{\mu,\downarrow}(\mathbf{r}_i, \tau) C_{\nu,\downarrow}(\mathbf{r}_i, \tau) C_{\nu,\uparrow}(\mathbf{r}_i, \tau) \right\} \right) \\ & = \int \mathcal{D}\bar{C}\mathcal{D}C \prod_{\mu} \mathcal{D}\bar{\Delta}_{\mu\mu}^{(1)} \mathcal{D}\Delta_{\mu\mu}^{(1)} \int \exp \left(\int_0^\beta d\tau \sum_{\mathbf{r}_i} \sum_{\mu \neq \nu} \left\{ \frac{3\bar{\Delta}_{\mu\mu}^{(1)}(\mathbf{r}_i, \tau) \Delta_{\mu\mu}^{(1)}(\mathbf{r}_i, \tau)}{W} + \frac{\bar{\Delta}_{\mu\mu}^{(1)}(\mathbf{r}_i, \tau) \Delta_{\nu\nu}^{(1)}(\mathbf{r}_i, \tau)}{W} \right\} \right. \\ & \quad \left. + \int_0^\beta d\tau \sum_{\mathbf{r}_i} \sum_{\mu \neq \nu} \left\{ \left[3\bar{\Delta}_{\mu\mu}^{(1)}(\mathbf{r}_i, \tau) + \bar{\Delta}_{\nu\nu}^{(1)}(\mathbf{r}_i, \tau) \right] C_{\mu,\downarrow}(\mathbf{r}_i, \tau) C_{\mu,\uparrow}(\mathbf{r}_i, \tau) \right. \right. \\ & \quad \left. \left. + \left[3\Delta_{\mu\mu}^{(1)}(\mathbf{r}_i, \tau) + \Delta_{\nu\nu}^{(1)}(\mathbf{r}_i, \tau) \right] \bar{C}_{\mu,\uparrow}(\mathbf{r}_i, \tau) \bar{C}_{\mu,\downarrow}(\mathbf{r}_i, \tau) \right\} \right), \end{aligned} \quad (\text{S11})$$

and the term

$$\begin{aligned} & \int \mathcal{D}\bar{C}\mathcal{D}C \exp \left(-W \int_0^\beta d\tau \sum_{\mathbf{r}_i} \sum_{\mu \neq \nu} \left[\bar{C}_{\mu,\uparrow}(\mathbf{r}_i, \tau) \bar{C}_{\nu,\downarrow}(\mathbf{r}_i, \tau) C_{\mu,\downarrow}(\mathbf{r}_i, \tau) C_{\nu,\uparrow}(\mathbf{r}_i, \tau) \right. \right. \\ & \quad \left. \left. + \bar{C}_{\mu,\uparrow}(\mathbf{r}_i, \tau) \bar{C}_{\nu,\downarrow}(\mathbf{r}_i, \tau) C_{\nu,\downarrow}(\mathbf{r}_i, \tau) C_{\mu,\uparrow}(\mathbf{r}_i, \tau) \right] \right), \end{aligned} \quad (\text{S12})$$

for instance, when considering $\mu, \nu = p_x, p_y$,

$$\begin{aligned}
& \int \mathcal{D}\bar{C}\mathcal{D}C \exp \left(-W \int_0^\beta d\tau \sum_{\mathbf{r}_i} \{ \bar{C}_{p_x, \uparrow}(\mathbf{r}_i, \tau) \bar{C}_{p_y, \downarrow}(\mathbf{r}_i, \tau) C_{p_x, \downarrow}(\mathbf{r}_i, \tau) C_{p_y, \uparrow}(\mathbf{r}_i, \tau) \right. \\
& \quad + \bar{C}_{p_y, \uparrow}(\mathbf{r}_i, \tau) \bar{C}_{p_x, \downarrow}(\mathbf{r}_i, \tau) C_{p_x, \downarrow}(\mathbf{r}_i, \tau) C_{p_y, \uparrow}(\mathbf{r}_i, \tau) + \bar{C}_{p_x, \uparrow}(\mathbf{r}_i, \tau) \bar{C}_{p_y, \downarrow}(\mathbf{r}_i, \tau) C_{p_y, \downarrow}(\mathbf{r}_i, \tau) C_{p_x, \uparrow}(\mathbf{r}_i, \tau) \\
& \quad \left. + \bar{C}_{p_y, \uparrow}(\mathbf{r}_i, \tau) \bar{C}_{p_x, \downarrow}(\mathbf{r}_i, \tau) C_{p_y, \downarrow}(\mathbf{r}_i, \tau) C_{p_x, \uparrow}(\mathbf{r}_i, \tau) \} \right) \\
& = \int \mathcal{D}\bar{C}\mathcal{D}C \prod_{j=1}^2 \mathcal{D}\bar{\Delta}_{p_x p_y}^{(j)} \mathcal{D}\Delta_{p_x p_y}^{(j)} \mathcal{D}\bar{\Delta}_{p_y p_x}^{(j)} \mathcal{D}\Delta_{p_y p_x}^{(j)} \exp \left(\frac{1}{W} \int_0^\beta d\tau \sum_{\mathbf{r}_i} \{ \bar{\Delta}_{p_y p_x}^{(2)}(\mathbf{r}_i, \tau) \Delta_{p_y p_x}^{(1)}(\mathbf{r}_i, \tau) + \bar{\Delta}_{p_x p_y}^{(1)}(\mathbf{r}_i, \tau) \Delta_{p_x p_y}^{(2)}(\mathbf{r}_i, \tau) \right. \\
& \quad + \bar{\Delta}_{p_y p_x}^{(1)}(\mathbf{r}_i, \tau) \Delta_{p_x p_y}^{(1)}(\mathbf{r}_i, \tau) + \bar{\Delta}_{p_x p_y}^{(2)}(\mathbf{r}_i, \tau) \Delta_{p_y p_x}^{(2)}(\mathbf{r}_i, \tau) \} + \int_0^\beta d\tau \{ [\Delta_{p_y p_x}^{(1)}(\mathbf{r}_i, \tau) + \Delta_{p_x p_y}^{(1)}(\mathbf{r}_i, \tau)] \bar{C}_{p_x, \uparrow}(\mathbf{r}_i, \tau) \bar{C}_{p_y, \downarrow}(\mathbf{r}_i, \tau) \\
& \quad + [\Delta_{p_y p_x}^{(2)}(\mathbf{r}_i, \tau) + \Delta_{p_x p_y}^{(2)}(\mathbf{r}_i, \tau)] \bar{C}_{p_y, \uparrow}(\mathbf{r}_i, \tau) \bar{C}_{p_x, \downarrow}(\mathbf{r}_i, \tau) + [\bar{\Delta}_{p_x p_y}^{(1)}(\mathbf{r}_i, \tau) + \bar{\Delta}_{p_y p_x}^{(1)}(\mathbf{r}_i, \tau)] C_{p_x, \downarrow}(\mathbf{r}_i, \tau) C_{p_y, \uparrow}(\mathbf{r}_i, \tau) \\
& \quad \left. + [\bar{\Delta}_{p_x p_y}^{(2)}(\mathbf{r}_i, \tau) + \bar{\Delta}_{p_y p_x}^{(2)}(\mathbf{r}_i, \tau)] C_{p_y, \downarrow}(\mathbf{r}_i, \tau) C_{p_x, \uparrow}(\mathbf{r}_i, \tau) \} \right). \tag{S13}
\end{aligned}$$

While in the case with $\mu, \nu = p_y, p_z$ and $\mu, \nu = p_x, p_z$, the corresponding expressions can be derived in the same way. We next introduce the following Fourier transformations

$$\begin{aligned}
C_{\mu, \mathbf{k}, n, \sigma} &= \frac{1}{\sqrt{\beta N}} \int_0^\beta \sum_{\mathbf{r}} C_{\mu, \sigma}(\mathbf{r}, \tau) e^{i\omega_n \tau - i\mathbf{k} \cdot \mathbf{r}} d\tau, & \bar{C}_{\mu, \mathbf{k}, n, \sigma} &= \frac{1}{\sqrt{\beta N}} \int_0^\beta \sum_{\mathbf{r}} \bar{C}_{\mu, \sigma}(\mathbf{r}, \tau) e^{-i\omega_n \tau + i\mathbf{k} \cdot \mathbf{r}} d\tau, \\
\Delta_{\mu\nu, \mathbf{q}, m}^{(j)} &= \frac{1}{\sqrt{\beta N}} \int_0^\beta \sum_{\mathbf{r}} \Delta_{\mu\nu}^{(j)}(\mathbf{r}, \tau) e^{i\varpi_m \tau - i\mathbf{q} \cdot \mathbf{r}} d\tau, & \bar{\Delta}_{\mu\nu, \mathbf{q}, m}^{(j)} &= \frac{1}{\sqrt{\beta N}} \int_0^\beta \sum_{\mathbf{r}} \bar{\Delta}_{\mu\nu}^{(j)}(\mathbf{r}, \tau) e^{-i\varpi_m \tau + i\mathbf{q} \cdot \mathbf{r}} d\tau, \tag{S14}
\end{aligned}$$

where N is the total number of lattice sites and $\omega_n = (2n+1)n/\beta$, $\varpi_m = 2m\pi/\beta$ with $\beta = 1/T$ are the fermionic and bosonic Matsubara frequencies, respectively. Since the superfluid state investigated here is the BCS-type, we can further approximately rewrite the Hubbard-Stratonovich fields representing the fermionic pairing as

$$\begin{aligned}
\Delta_{\mu\nu, \mathbf{q}, m}^{(j)} &= \sqrt{\beta N} \delta_{\mathbf{q}, 0} \delta_{m, 0} \Delta_{\mu\nu}^{(j)}, \\
\bar{\Delta}_{\mu\nu, \mathbf{q}, m}^{(j)} &= \sqrt{\beta N} \delta_{\mathbf{q}, 0} \delta_{m, 0} \bar{\Delta}_{\mu\nu}^{(j)}. \tag{S15}
\end{aligned}$$

Then the partition function becomes

$$\mathcal{Z} = \int \mathcal{D} \{ \bar{C}, C, \bar{\Delta}^{(j)}, \Delta^{(j)} \} \exp \left(-S_{sp} \left[\bar{C}, C, \bar{\Delta}^{(j)}, \Delta^{(j)} \right] \right),$$

$$\begin{aligned}
S_{sp} [\bar{C}, C, \bar{\Delta}, \Delta] = & -\frac{N\beta}{W} \sum_{\mu \neq \nu} \left(3\bar{\Delta}_{\mu\mu}^{(1)} \Delta_{\mu\mu}^{(1)} + \bar{\Delta}_{\mu\mu}^{(1)} \Delta_{\nu\nu}^{(1)} \right) - \frac{N\beta}{W} \sum_{\substack{\mu\nu=\{p_x p_y, \\ p_y p_z, p_z p_x\}}} \left(\bar{\Delta}_{\mu\nu}^{(1)} \Delta_{\mu\nu}^{(2)} + \bar{\Delta}_{\nu\mu}^{(2)} \Delta_{\nu\mu}^{(1)} + \bar{\Delta}_{\nu\mu}^{(1)} \Delta_{\mu\nu}^{(1)} + \bar{\Delta}_{\mu\nu}^{(2)} \Delta_{\nu\mu}^{(2)} \right) \\
& + \sum_{\mathbf{k}, n, \mu, \nu, \sigma} \bar{C}_{\mu, \mathbf{k}, n, \sigma} \left(-i\omega_n \delta_{\mu\nu} + [\mathcal{H}(\mathbf{k})]_{\mu\nu} \right) C_{\nu, \mathbf{k}, n, \sigma} - \sum_{\substack{\mathbf{k}, n \\ \mu \neq \nu}} \left([3\bar{\Delta}_{\mu\mu}^{(1)} + \bar{\Delta}_{\nu\nu}^{(1)}] C_{\mu, -\mathbf{k}, -n, \downarrow} C_{\mu, \mathbf{k}, n, \uparrow} \right. \\
& + [3\Delta_{\mu\mu}^{(1)} + \Delta_{\nu\nu}^{(1)}] \bar{C}_{\mu, \mathbf{k}, n, \uparrow} \bar{C}_{\mu, -\mathbf{k}, -n, \downarrow} \left. - \sum_{\substack{\mathbf{k}, n \\ \mu\nu=\{p_x p_y, \\ p_y p_z, p_z p_x\}}} \left([\bar{\Delta}_{\mu\nu}^{(1)} + \bar{\Delta}_{\nu\mu}^{(1)}] C_{\mu, -\mathbf{k}, -n, \downarrow} C_{\nu, \mathbf{k}, n, \uparrow} \right. \right. \\
& + [\Delta_{\mu\nu}^{(1)} + \Delta_{\nu\mu}^{(1)}] \bar{C}_{\mu, \mathbf{k}, n, \uparrow} \bar{C}_{\nu, -\mathbf{k}, -n, \downarrow} \left. - \sum_{\substack{\mathbf{k}, n \\ \mu\nu=\{p_y p_x, \\ p_z p_y, p_x p_z\}}} \left([\bar{\Delta}_{\mu\nu}^{(2)} + \bar{\Delta}_{\nu\mu}^{(2)}] C_{\mu, -\mathbf{k}, -n, \downarrow} C_{\nu, \mathbf{k}, n, \uparrow} \right. \right. \\
& \left. \left. + [\Delta_{\mu\nu}^{(2)} + \Delta_{\nu\mu}^{(2)}] \bar{C}_{\mu, \mathbf{k}, n, \uparrow} \bar{C}_{\nu, -\mathbf{k}, -n, \downarrow} \right) \right). \tag{S16}
\end{aligned}$$

We then further represent the action in Nambu representation

$$\begin{aligned}
S_{sp} [\bar{C}, C, \bar{\Delta}, \Delta] = & -\frac{N\beta}{W} \sum_{\mu \neq \nu} \left(3\bar{\Delta}_{\mu\mu}^{(1)} \Delta_{\mu\mu}^{(1)} + \bar{\Delta}_{\mu\mu}^{(1)} \Delta_{\nu\nu}^{(1)} \right) - \frac{N\beta}{W} \sum_{\substack{\mu\nu=\{p_x p_y, \\ p_y p_z, p_z p_x\}}} \left(\bar{\Delta}_{\mu\nu}^{(1)} \Delta_{\mu\nu}^{(2)} + \bar{\Delta}_{\nu\mu}^{(2)} \Delta_{\nu\mu}^{(1)} + \bar{\Delta}_{\nu\mu}^{(1)} \Delta_{\mu\nu}^{(1)} + \bar{\Delta}_{\mu\nu}^{(2)} \Delta_{\nu\mu}^{(2)} \right) \\
& + \sum_{\mathbf{k}, n} \bar{\eta}_{\mathbf{k}, n} \left(-i\omega_n \mathbb{I}_6 + H_{BdG}(\mathbf{k}) \right) \eta_{\mathbf{k}, n}, \tag{S17}
\end{aligned}$$

where $\eta_{\mathbf{k}, n} = \left(C_{p_x, \mathbf{k}, n, \uparrow} \ C_{p_y, \mathbf{k}, n, \uparrow} \ C_{p_z, \mathbf{k}, n, \uparrow} \ \bar{C}_{p_x, -\mathbf{k}, -n, \downarrow} \ \bar{C}_{p_y, -\mathbf{k}, -n, \downarrow} \ \bar{C}_{p_z, -\mathbf{k}, -n, \downarrow} \right)^T$ is the Nambu spinor. \mathbb{I}_6 is the 6×6 unit matrix and $H_{BdG}(\mathbf{k})$ is the 6×6 Bogoliubov-de Gennes matrix

$$H_{BdG}(\mathbf{k}) = \begin{pmatrix} \mathcal{H}(\mathbf{k}) & -M \\ -\bar{M} & -\mathcal{H}^T(-\mathbf{k}) \end{pmatrix},$$

$$M = \begin{pmatrix} 3\Delta_{p_x p_x}^{(1)} + \Delta_{p_y p_y}^{(1)} + \Delta_{p_z p_z}^{(1)} & \Delta_{p_x p_y}^{(1)} + \Delta_{p_y p_x}^{(1)} & \Delta_{p_x p_z}^{(2)} + \Delta_{p_z p_x}^{(2)} \\ \Delta_{p_x p_y}^{(2)} + \Delta_{p_y p_x}^{(2)} & 3\Delta_{p_y p_y}^{(1)} + \Delta_{p_x p_x}^{(1)} + \Delta_{p_z p_z}^{(1)} & \Delta_{p_y p_z}^{(1)} + \Delta_{p_z p_y}^{(1)} \\ \Delta_{p_x p_z}^{(1)} + \Delta_{p_z p_x}^{(1)} & \Delta_{p_y p_z}^{(2)} + \Delta_{p_z p_y}^{(2)} & 3\Delta_{p_z p_z}^{(1)} + \Delta_{p_x p_x}^{(1)} + \Delta_{p_y p_y}^{(1)} \end{pmatrix},$$

with

$$\bar{M} = \begin{pmatrix} 3\bar{\Delta}_{p_x p_x}^{(1)} + \bar{\Delta}_{p_y p_y}^{(1)} + \bar{\Delta}_{p_z p_z}^{(1)} & \bar{\Delta}_{p_x p_y}^{(1)} + \bar{\Delta}_{p_y p_x}^{(1)} & \bar{\Delta}_{p_x p_z}^{(2)} + \bar{\Delta}_{p_z p_x}^{(2)} \\ \bar{\Delta}_{p_x p_y}^{(2)} + \bar{\Delta}_{p_y p_x}^{(2)} & 3\bar{\Delta}_{p_y p_y}^{(1)} + \bar{\Delta}_{p_x p_x}^{(1)} + \bar{\Delta}_{p_z p_z}^{(1)} & \bar{\Delta}_{p_y p_z}^{(1)} + \bar{\Delta}_{p_z p_y}^{(1)} \\ \bar{\Delta}_{p_x p_z}^{(1)} + \bar{\Delta}_{p_z p_x}^{(1)} & \bar{\Delta}_{p_y p_z}^{(2)} + \bar{\Delta}_{p_z p_y}^{(2)} & 3\bar{\Delta}_{p_z p_z}^{(1)} + \bar{\Delta}_{p_x p_x}^{(1)} + \bar{\Delta}_{p_y p_y}^{(1)} \end{pmatrix}. \tag{S18}$$

Integrating out the fermionic fields, the partition function can be expressed as

$$\mathcal{Z} = \exp \left(-\beta N F_{sp}(\bar{\Delta}, \Delta, T, \mu) \right), \tag{S19}$$

$$\begin{aligned}
F_{sp}(\bar{\Delta}, \Delta, T, \mu) = & -\frac{1}{W} \sum_{\mu \neq \nu} \left(3\bar{\Delta}_{\mu\mu}^{(1)} \Delta_{\mu\mu}^{(1)} + \bar{\Delta}_{\mu\mu}^{(1)} \Delta_{\nu\nu}^{(1)} \right) - \frac{1}{W} \sum_{\substack{\mu\nu=\{p_x p_y, \\ p_y p_z, p_z p_x\}}} \left(\bar{\Delta}_{\mu\nu}^{(1)} \Delta_{\mu\nu}^{(2)} + \bar{\Delta}_{\nu\mu}^{(2)} \Delta_{\nu\mu}^{(1)} + \bar{\Delta}_{\nu\mu}^{(1)} \Delta_{\mu\nu}^{(1)} + \bar{\Delta}_{\mu\nu}^{(2)} \Delta_{\nu\mu}^{(2)} \right) \\
& - \frac{1}{N\beta} \sum_{\mathbf{k}, n} \ln \left\{ -\det \left[-i\omega_n \mathbb{I}_6 + H_{BdG}(\mathbf{k}) \right] \right\}. \tag{S20}
\end{aligned}$$

Then the filling of the system and the saddle values of the Hubbard-Stratonovich fields representing the fermionic pairing can be determined by

$$n = -\frac{\partial F_{sp}(\bar{\Delta}, \Delta, T, \mu)}{\partial \mu}, \quad \frac{\partial F_{sp}(\bar{\Delta}, \Delta, T, \mu)}{\partial \bar{\Delta}_{\mu\nu}^{(j)}} = 0, \quad \frac{\partial F_{sp}(\bar{\Delta}, \Delta, T, \mu)}{\partial \Delta_{\mu\nu}^{(j)}} = 0. \tag{S21}$$

From Eq. (S21), we can define the pairing order parameters as $\Delta_{\mu\nu} \equiv \Delta_{\mu\nu}^{(1)}, \Delta_{\mu\nu}^* \equiv \bar{\Delta}_{\mu\nu}^{(1)}$ when $\mu = \nu$, and for $\mu \neq \nu$, $\Delta_{\mu\nu} \equiv \Delta_{\mu\nu}^{(1)} = \Delta_{\mu\nu}^{(2)}, \Delta_{\mu\nu}^* \equiv \bar{\Delta}_{\mu\nu}^{(1)} = \bar{\Delta}_{\mu\nu}^{(2)}$. Therefore, we can rewrite the $H_{BdG}(\mathbf{k})$ as

$$H_{BdG}(\mathbf{k}) = \begin{pmatrix} \mathcal{H}(\mathbf{k}) & -M \\ -(M^T)^* & -\mathcal{H}^T(-\mathbf{k}) \end{pmatrix},$$

$$M = \begin{pmatrix} 3\Delta_{p_x p_x} + \Delta_{p_y p_y} + \Delta_{p_z p_z} & \Delta_{p_x p_y} + \Delta_{p_y p_x} & \Delta_{p_x p_z} + \Delta_{p_z p_x} \\ \Delta_{p_x p_y} + \Delta_{p_y p_x} & 3\Delta_{p_y p_y} + \Delta_{p_x p_x} + \Delta_{p_z p_z} & \Delta_{p_y p_z} + \Delta_{p_z p_y} \\ \Delta_{p_x p_z} + \Delta_{p_z p_x} & \Delta_{p_y p_z} + \Delta_{p_z p_y} & 3\Delta_{p_z p_z} + \Delta_{p_x p_x} + \Delta_{p_y p_y} \end{pmatrix}. \quad (\text{S22})$$

S-4. BEREZINSKII-KOSTERLITZ-THOULESS (BKT) TRANSITION

It is well known that at finite temperature the superfluidity of 2D atomic Fermi gases is characterized by the vortex-antivortex binding. The relevant mechanism is the Berezinskii-Kosterlitz-Thouless (BKT) [51, 52] transition occurring at a characteristic temperature T_{BKT} . The BKT transition in 2D is associated with the spontaneous vortex formation. A unique feature of such a transition is an universal jump in the superfluid density [59]. To further determine the superfluid density, we imposing a phase twist (e.g. see [60–62]), i.e., a supercurrent, on the order parameter as

$$\Delta_{\mu\nu} \rightarrow \Delta_{\mu\nu} \exp(i \cdot 2\Theta \cdot \mathbf{r}_i) = \Delta_{\mu\nu} \exp\left(i \frac{2\Theta_x n_x}{N_x} + i \frac{2\Theta_y n_y}{N_y}\right), \quad (\text{S23})$$

where $\mathbf{r}_i = n_x a \vec{e}_x + n_y a \vec{e}_y$ labels the lattice site. Θ captures the linear phase variation on the order parameter and N_x, N_y represents the site number along x and y direction, respectively. This imposed phase gradient gives the system a kinetic energy, which corresponds to the free energy difference $\Delta F \equiv F_\Theta - F_0$, where F_Θ is the free energy within the phase variation and F_0 is the free energy without the phase variation. We then approximate ΔF up to the second order in Θ as $\Delta F \simeq \sum_{\alpha, \beta=x, y} F_{\alpha\beta}^{(2)} \Theta_\alpha \Theta_\beta$. Due to the reflection symmetry of the system, when $\alpha \neq \beta$, $F_{\alpha\beta}^{(2)}$ vanishes and we further have

$$F_{\alpha\alpha}^{(2)} = \frac{T}{2N} \sum_{\mathbf{k}, n, \mu, \nu} \left[\frac{\partial^2 \mathcal{H}(\mathbf{k})}{\partial^2 k_\alpha} \right]_{\mu\nu} \left(-[G_{\mathbf{k}, n, \uparrow}]_{\nu\mu} - [G_{-\mathbf{k}, -n, \downarrow}]_{\mu\nu} \right)$$

$$+ \frac{T}{2} \sum_{\mathbf{k}, n, \mu, \nu, \mu', \nu'} \left[\frac{\partial \mathcal{H}(\mathbf{k})}{\partial k_\alpha} \right]_{\mu\nu} \left[\frac{\partial \mathcal{H}(\mathbf{k})}{\partial k_\alpha} \right]_{\mu'\nu'} \left([G_{\mathbf{k}, n, \uparrow}]_{\nu\mu'} [G_{\mathbf{k}, n, \uparrow}]_{\nu'\mu} + [G_{\mathbf{k}, n, \downarrow}]_{\nu\mu'} [G_{\mathbf{k}, n, \downarrow}]_{\nu'\mu} \right)$$

$$+ [F_{\mathbf{k}, n}]_{\nu\mu'} [F_{\mathbf{k}, n}^\dagger]_{\nu'\mu} + [F_{\mathbf{k}, n}]_{\nu'\mu} [F_{\mathbf{k}, n}^\dagger]_{\nu\mu'} \Big), \quad (\text{S24})$$

with $[G_{\mathbf{k}, n, \sigma}]_{\mu\nu} = \langle C_{\mu, \mathbf{k}, n, \sigma} \bar{C}_{\nu, \mathbf{k}, n, \sigma} \rangle$ and $[F_{\mathbf{k}, n}]_{\mu\nu} = \langle C_{\mu, \mathbf{k}, n, \uparrow} C_{\nu, -\mathbf{k}, -n, \downarrow} \rangle$ are matrix elements of the normal and anomalous Greens's functions. Then the BKT transition temperature can be determined through $k_B T_{BKT} = \frac{\pi}{4} F^{(2)}$ with $F^{(2)} \equiv (F_{xx}^{(2)} + F_{yy}^{(2)})/2$.